Journal of Power Sources 286 (2015) 103–108

Contents lists available at ScienceDirect

Journal of Power Sources

journal homepage: www.elsevier.com/locate/jpowsour

Stability of carbon nanotube yarn biofuel cell in human body fluid

Cheong Hoon Kwon [a], Jae Ah Lee [a], Young-Bong Choi [b], Hyug-Han Kim [b], Geoffrey M. Spinks [c], Márcio D. Lima [d], Ray H. Baughman [d], Seon Jeong Kim [a, *]

[a] Center for Bio-Artificial Muscle and Department of Biomedical Engineering, Hanyang University, Seoul, 133-791, Republic of Korea
[b] Department of Chemistry, Dankook University, Cheonan, Choongnam, 330-714, Republic of Korea
[c] Intelligent Polymer Research Institute, ARC Centre of Excellence for Electromaterials Science, University of Wollongong, Wollongong, NSW, 2522, Australia
[d] The Alan G. MacDiarmid NanoTech Institute, University of Texas at Dallas, Richardson, TX 75083, USA

HIGHLIGHTS

- A yarn-type enzymatic biofuel cell was developed with enhanced long-term (>20 days) stability.
- Enzymatic biofuel cell generates an open circuit voltage of 0.80 V in human blood serum.
- The maximum power density of 1.1 mW cm^{-2} was obtained at an operating voltage of 0.50 V in human blood serum.

ARTICLE INFO

Article history:
Received 16 December 2014
Received in revised form
27 January 2015
Accepted 23 March 2015
Available online 24 March 2015

Keywords:
Biofuel cell
Human blood serum
Stability
Carbon nanotube
Flexibility

ABSTRACT

High performance with stability, easy-handling electrodes, and biofluid-flow controllable system with mechanical strength of the biofuel cell can be considered as the critical issues for future human body implant. These three challenges are sufficiently considered by using the effective platform regarding the high surface area from multi-walled carbon nanotube-conducting polymer with poly(3,4-ethylenedioxythiophene), and size/shape dependent flexible yarn electrodes for the implantation of biofuel cell. High power biofuel cell of mW cm^{-2} range in physiological condition (low glucose-containing phosphate buffered saline solution and human blood serum) controlling the stirring degree is also first demonstrated for future implantation in this study. Biofuel cells for future implantation in human body vitally require long-term stability and high power outputs. We have demonstrated that a high-surface area yarn-based biofuel cell retained over 70% of its initial power output after an extended 20 days period of continuous operation in human blood serum, while delivering a power density of ~1.0 mW cm^{-2}. Subsequently, our enhanced enzymatic biofuel cell system would be potentially used as an innovative power source for the next generation implantable electronics.

1. Introduction

Biofuel cells (BFCs) are of great interest as power sources for implanted miniaturized biomedical devices since they offer continuous power supply through conversion of biochemical fuels, such as glucose [1]. Implantable electrodes (or devices) need to satisfy many criteria such as biocompatibility, miniaturization, easy-handling, robustness, high power output, high durability, and long-term stability.

To date, the best performing BFCs operating in near physiological conditions have generated a power density of the order of 1 mW cm^{-2}. Kim and Yoo have reported an output of 0.64 mW cm^{-2} in serum condition that operated stably for eight days [2]. In another recent result, a maximum power density of 0.11 mW cm^{-2} was reported in human serum (10 mM glucose solution) [3]. We have recently also reported a BFC operating for 2 days and producing ~1 mW cm^{-2} in both low concentration glucose, 7 mM, in phosphate buffered saline (PBS) and in human blood serum (HBS) [4]. Power generation was even lower in implanted BFC operating in a live cockroach [5]. Under 50 mM trehalose in PBS solution and cockroach hemolymph (ca. 5%) the power outputs were 15 μW cm^{-2} and 55 μW cm^{-2}, respectively.

Enzyme-loaded BFC electrodes tend to suffer degradation due to the presence of chemical species, such as urate, chloride ion, and ascorbic acid which exist at high level in the biological systems like

* Corresponding author.
E-mail address: sjk@hanyang.ac.kr (S.J. Kim).

http://dx.doi.org/10.1016/j.jpowsour.2015.03.140
0378-7753/

HBS [6]. Urate induces remarkable deactivation of bilirubin oxidase as commonly used in the BFC cathode and ascorbic acid decreases the open circuit voltage. As a consequence, BFC performance can deteriorate within hours of operation in physiological conditions. Our enzymatic BFC system was effectively operated with no significant performance loss and stability decline for two days in HBS. The electrodes consist of porous yarns of multi-walled carbon nanotubes (MWNT) coated in poly(3,4-ethylenedioxythiophene) (PEDOT) and incorporating electrode specific enzymes and redox mediators. The high stability and tolerance to antagonistic chemical species was ascribed to the cation-exchange nature of the PEDOT that reduced the rate of degradation without compromising electrode conductivity [4]. These fiber type electrodes have high surface area to volume ratios and can be assembled into compact, robust systems, such as woven textiles [4]. These characteristics favorably compared with film [7] or disk [8] type electrodes that can have relatively low volumetric power density and can be difficult to insert and handle.

BFC power output is dependent on glucose concentration which is also related to blood flow rates in implanted devices. We have shown in our recent study [4] that power output can be doubled by increasing the glucose concentration from 7 mM to 60 mM in PBS. Normal blood flows are very different around major organs such as the heart, liver, or kidney [9]. Yet only a few studies have reported on the effect of biofluid flow on BFC power output [10,11]. In one recent example, an implantable biofuel cell system was used with lobsters [12] to mimic human blood circulation for a resting person (58.9 μl min^{-1}) and a person performing physical activity (235.6 μl min^{-1}). These markedly different flow rates highlight the importance of characterizing BFC performance under different flow conditions, such as by varying stirring speeds.

Here we investigate further the BFC performance in physiological conditions of the MWNT/PEDOT yarn based enzymatic electrodes. In particular, we consider the effect of electrolyte flow rate on BFC power output to determine the likely influence of varying blood flow rates. Secondly, we evaluate the performance of the BFC during continuous operation up to 20 days.

2. Experimental

2.1. Materials

MWNT forests (~400 mm high and consisting of ~12 nm diameter nanotubes) were grown on a Si wafer by chemical vapor deposition. PVA (Mw 146,000–186,000), iron(III) p-toluenesulfonate hexahydrate (Fe(III)PTS), pyridine (anhydrous, 99.8% purity), 1-butanol (~99% purity) and 3,4-ethylenedioxythiophene (EDOT, 97% purity) were from Sigma–Aldrich Corporation and 1 M aqueous sulfuric acid solution was from Daejung Chemicals and Metals Company. The guests of BFC electrode consist of redox mediator, enzyme, and cross-linker. The anodic redox mediator I was PVI-Os(dmo-bpy)$_2$Cl$^{+/2+}$, poly(N-vinylimidazole)-[Os(4,4′-dimethoxy-2,2′-bipyridine)$_2$Cl])$^{+/2+}$, and the cathodic redox mediator II was PAA-PVI-Os(dCl-bpy)$_2$Cl$^{+/2+}$, poly(acryl amide)-poly(N-vinylimidazole)-[Os(4,4′-dichloro-2,2′-bipyridine)$_2$])$^{+/2+}$. Glucose oxidase (GOx) from *aspergillus niger* (219 U mg^{-1}) from Amano Enzyme Inc. (Japan) was used as an anodic enzyme. Bilirubin oxidase (BOD) from *myrothecium verrucaria* (10.5 U mg^{-1}, Sigma Aldrich was used as a cathodic catalyst. Poly(ethylene glycol) diglycidyl ether (PEGDGE) from Polysciences, Inc was used to cross-link each enzymes and redox mediators. Human blood serum (HBS) was purchased from Biological Specialty, USA. Glucose level of HBS was 4 mM–7 mM, as they reported.

2.2. Characterizations and electrochemical measurements

Surface morphologies of BFC electrode were characterized using scanning electron microscopy (Hitachi S4700). For electrochemical measurements, linear sweep voltammetry was obtained using electrochemical analyzing system (CHI 627B from CH Instruments). A three-electrode electrochemical system was used for cyclic voltammetry and chronoamperometry. A biscrolled yarn electrode was used as the working electrode, with Ag/AgCl reference electrode and a Pt mesh counter electrode. The measurements were conducted at 37 °C under the same condition with the human body in an electrochemical cell containing 50 mL PBS solution (20 mM phosphate, 0.14 M NaCl, pH: ~7.4) or HBS.

2.3. Fabrication of BFC biscrolled yarn electrodes

Biscrolled yarn was fabricated with a PEDOT-coated MWNT sheet and guest materials. Guests-filled PEDOT-coated MWNT sheet was slowly twisted using the motor with ~5000 turns per meter of inserted twist per yarn length. After twist insertion, both ends of the biscrolled yarn were fixed to the glass slide using carbon tape and BFC biscrolled yarn was cured at 4 °C for 24 h. Both the anodic yarn electrode (3.5-mm-long, 90-μm-diameter) and the cathodic yarn electrode (4.0-mm-long, 80-μm-diameter) were used and an active external surface area was 1.01 mm^2 for this study.

3. Results and discussion

3.1. Yarn-based anodic and cathodic electrode performance considering the flow of human body fluids

The complete BFC system is introduced in Fig. 1. PEDOT-coated MWNT sheets was used as a host material for our enzymatic BFC system. This PEDOT-coated MWNT sheet was dipped into each guest solution specifically developed for anodic and cathodic electrodes (Fig. 1a). Twisting the sheet (Fig. 1b) completed the fabrication of the biscrolled yarn electrodes for both anode and cathode. Scanning electron microscopy (SEM) image shows BFC electrode surface in Fig. 1c revealing the PEDOT-coated MWNT bundles. Enlarged surface and cross-section images are shown in Fig. 1d,e. The cross-section clearly shows the porous vascular structure that is important for fast mass transport of the fuels, glucose and oxygen, to the reaction centres imbibed within the PEDOT coating.

The electrochemical characterization of the enzymatic BFC electrodes were measured in two buffer conditions, PBS containing low glucose and HBS, and at different stirring rates. Anodic current densities were measured at various glucose concentrations from 0 to 15 mM in PBS (Fig. 2a). Power densities increased almost linearly with glucose concentration over this range. Higher power outputs at a given glucose concentration were achieved with more intense stirring of the buffer solution. Linear sweep voltammetry was conducted at a glucose concentration of 7 mM, which is similar to that of HBS. The linear sweep clearly show the current limited by concentration polarization at potentials above ~0.05 V. The maximum anodic current densities were higher in PBS than in HBS and increased by moderate stirring at 500 rpm. The maximum current density (from the average value of the range between +0.2 V and +0.4 V), as shown in Fig. 2b was 4.7 mA cm^{-2} without any stirring effect and 5.5 mA cm^{-2} with 500 rpm in PBS containing 7 mM glucose fuel, and 4.0 and 5.2 mA cm^{-2} in HBS. These current densities are relatively high compared to the previously reported result of 0.6 mA cm^{-2} under physiological condition (quiescent solution, air, PBS buffer, 15 mM glucose, 37 °C) [13].

Cathodic current density performance is shown in Fig. 3a.

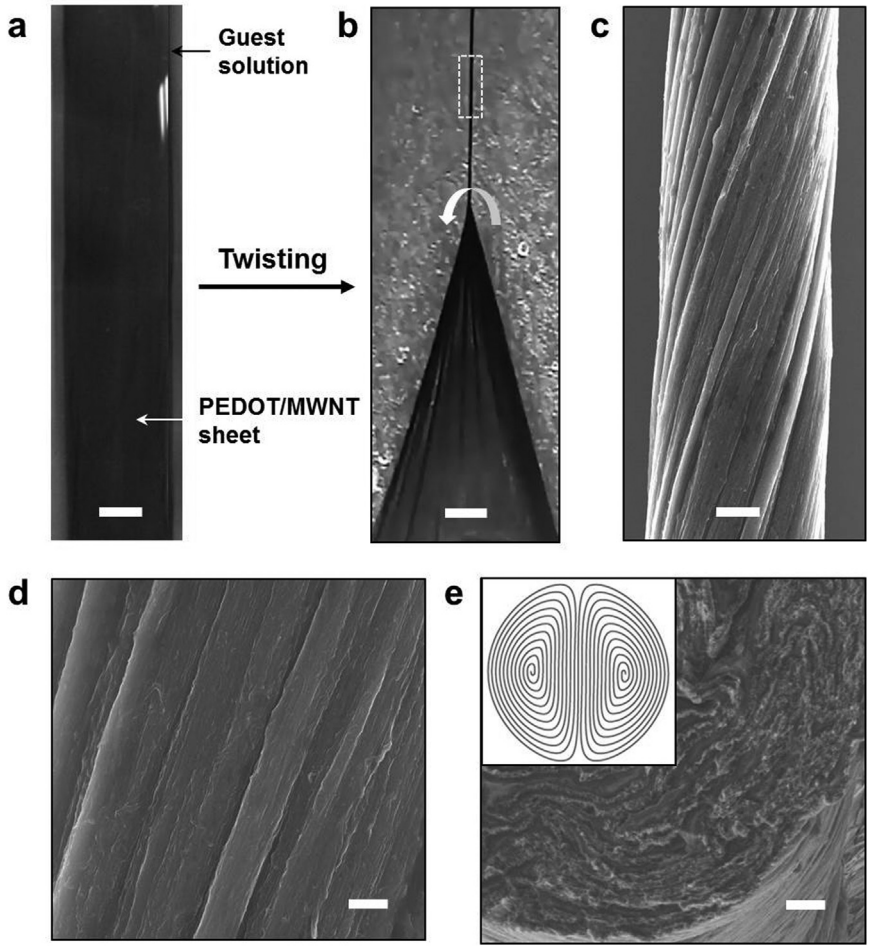

Fig. 1. Yarn-based enzymatic BFC electrode. a) Deposition of guest materials, such as enzyme, redox mediator, and cross-linker on the PEDOT/MWNT sheet. Scale bar is 3 mm. b) Optical image of twisting process for fabricating the biscrolled yarn electrode. Scale bar is 1.5 mm. The fabricated biscrolled yarn electrode (indicated by white color, dashed square) was enlarged in Fig. 1c. c) SEM micrograph showing the surface of BFC yarn cathode electrode (Scale bar: 20 μm). d) Enlarged SEM image of surface morphology. Scale bar, 2 μm. e) SEM cross-section image of three dimensional BFC yarn electrode structure (Scale bar: 5 μm). The inset illustrates a dual Archimedean scroll.

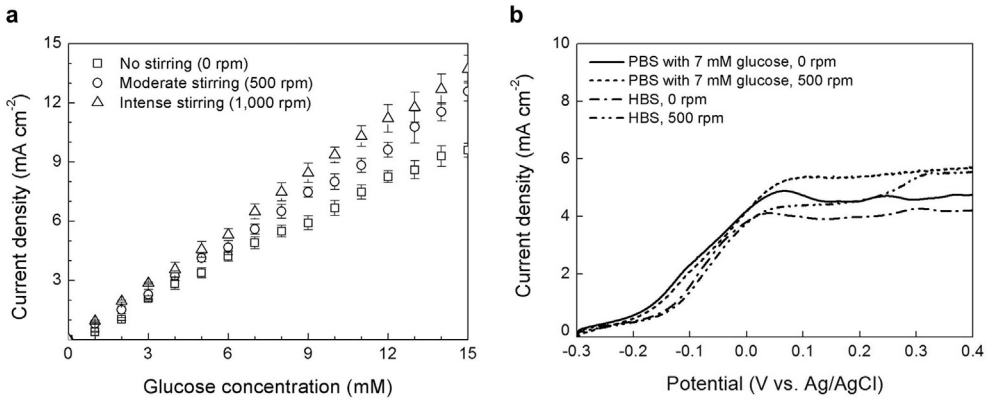

Fig. 2. Anodic performance depending on the stirring degree in physiological conditions. a) Anodic current density changes according to the concentration of the glucose fuel from 0 to 15 mM with three stirring conditions, 0 rpm, 500 rpm, and 1000 rpm. The error bars show the s.d. from the current densities for three independent experiments. b) Polarization curves of the anodic current densities under PBS containing 7 mM glucose and HBS with no stirring and 500 rpm.

Without any stirring, a maximum current density of 2.3 mA cm^{-2} in PBS with 7 mM glucose fuel and 2.2 mA cm^{-2} in HBS were obtained from the average value of the range between −0.1 V and +0.1 V.

These values increased under mild stirring (500 rpm) to 3.1 mA cm^{-2} in PBS with 7 mM glucose fuel and 2.8 mA cm^{-2} in HBS. Current densities of cathode were further increased by increasing the stirring degree from 0 to 1000 rpm, as shown in Fig. 3b. With the stirring of 1000 rpm, the cathodic current

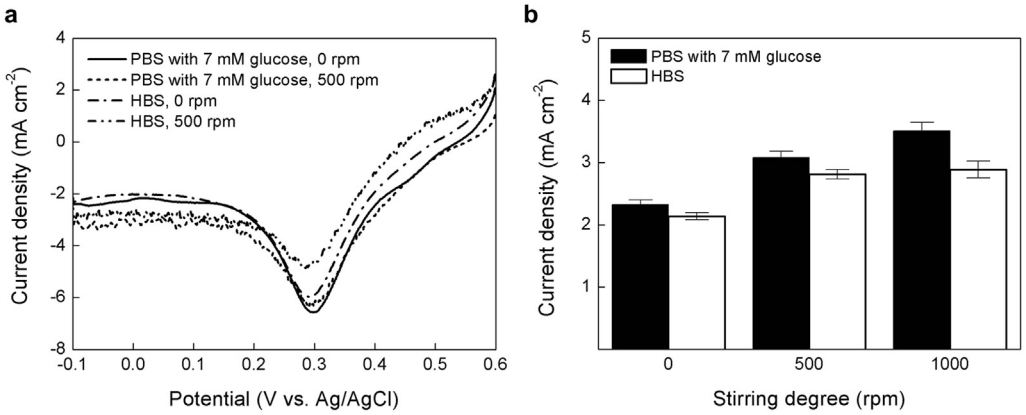

Fig. 3. Cathodic performance depending on the stirring degree in physiological conditions. a) Polarization curves of the cathodic current densities under PBS containing 7 mM glucose and HBS with no stirring and 500 rpm. b) Maximum current density changes by stirring (0, 500, and 1000 rpm) in 7 mM glucose-containing PBS buffer and HBS. The error bars show the s.d. from the current densities for three experiments.

densities of 3.5 mA cm^{-2} in PBS with 7 mM glucose fuel, and 2.9 mA cm^{-2} in HBS were acquired. The more stirring degree was increased, the more cathodic current density was increased and respective error was also inclined to increase [14].

The electrocatalytic behaviors were investigated by means of cyclic voltammetry (Supporting Information, Fig. S1) and electrochemical impedance spectroscopy (Supporting Information, Fig. S2). The impedance spectra shapes were similar for both anode and cathode, and the electron-transfer resistances correspond to ~175 Ω, for anode and ~286 Ω for cathode, respectively. These electron-transfer resistances of the biofuel cell represent the internal resistances of the biscrolled yarn electrode containing different enzyme under the physiologically relevant operating conditions.

3.2. Power output based on the body fluid flow

Power density curves of our BFC in a quiescent solution are shown in Fig. 4a. A maximum power density of 1.2 mW cm^{-2} was obtained at an operating voltage of 0.46 V when using 7 mM glucose PBS buffer, and 1.1 mW cm^{-2} was obtained at 0.50 V in HBS. Open circuit voltage was 0.83 V and 0.80 V, respectively, in these two physiological conditions. The open circuit voltage in generally lower than that under glucose-containing PBS buffer condition, according to the reports [15]. It was previously demonstrated with two reasons, oxygen concentration for cathode fuel is very low, compared to PBS solution, and the dissolved oxygen may partially react with glucose at the anode. (Isolating the anode and cathode fluid, and removing the oxygen from anode fluid will improve the open circuit voltage, but it is difficult to achieve it in implanted devices, using both oxygen and glucose from the same biofluid.) The obtained 1.1 mW cm^{-2} maximum power density is higher than a reported maximum power density (0.64 mW cm^{-2}) [2] in serum containing 10 mM glucose solution, at the scan rate of 40 mV s^{-1}. In addition, the volumetric power densities were 278 mW cm^{-3} and 252 mW cm^{-3}, in 7 mM glucose-containing PBS solution and HBS, respectively. Additionally, our gravimetric power outputs were 95 mW g^{-1} in 7 mM, without stirring.

In Fig. 4b, power densities obtained by changing the stirring ratio and representing the effect of varying blood flow rates are represented. As increasing the stirring degree from 0 to 1000 rpm, power density was also increased, up to 1.6 mW cm^{-2} in low glucose-containing PBS buffer and 1.2 mW cm^{-2} in HBS, respectively. These stirring degree-dependent power output are relevant since the flow rate of fluids in animals or humans varies throughout the body (for example, 0.5 L min^{-1} near liver, 0.55 L min^{-1} near

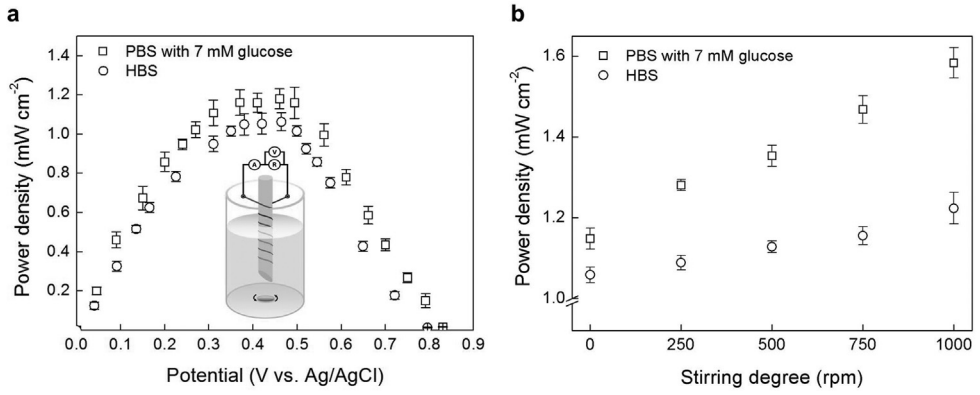

Fig. 4. Enzymatic BFC power densities in physiological conditions. The error bars show the s.d. from the power densities for three cases. a) Power densities of BFC without stirring under physiological conditions (7 mM glucose-containing PBS and HBS). Inset: Complete BFC system consisting of anode and cathode yarn parallel wrapped around a glass rod to avoid short circuiting, immersed in HBS and continuously operated at 37 °C with stirring. b) Power density changes by increasing the stirring degree from 0 to 1000 rpm, at an interval of 250 rpm, in glucose-containing PBS buffer and HBS.

kidney, and 5.25 L min^{-1} near heart of human body [9]).

This exceptional performance realized for the biscrolled yarn BFC results in part from the yarn's three-dimensional vascular structure. The corridors between scrolled PEDOT/MWNT sheets in the biscrolled yarn provide a continuous internal pathway for rapid glucose and oxygen diffusion and ion transport from yarn surface to yarn center, as well as sufficient porosity through scroll layers for cross-layer transport. Our enzymatic BFCs describing high power output performance in physiological conditions (glucose-containing PBS buffer and human body fluid) contribute to provide feasible power source for energy generation considering future human body implants.

3.3. Enzymatic BFC stability in HBS

BFC stability is considered as a critical issue related to the effective enzyme immobilization for both anode and cathode. In most previous studies, the enzymatic electrodes in HBS showed rapid deterioration within a few hours of operation [16,17]. Reversible deactivation and irreversible damage of bio-cathode could also decrease the stability of the BFC device. Attempts to improve the stability of enzymatic BFCs have resulted in recently reported BFC (0.64 mW cm^{-2}) [2] in serum condition provided the stability for eight days, while another work (0.11 mW cm^{-2}) [3] showed only 43% stability based on the remaining percentage from the initial power density value after 3 days.

Previous investigations of enzymatic PEDOT/MWNT yarn type BFCs were restricted to 2 days of continuous operation. Here the time dependence of the power density of the cell poised at 0.40 V in 7 mM glucose-containing PBS solution and HBS under air at 37 °C is shown in Fig. 5a. Based on the initial power density, the BFC retained 81% of power density in PBS under 7 mM glucose buffer solution, and 72% in HBS after 10 days with continuous operating. After 20 days, the power outputs of biofuel cell remained at 80% and 71% in 7 mM glucose-containing PBS and HBS, respectively. After 28 days of continuous operation the retained power densities were ~77% for glucose-containing PBS buffer, and ~68% for HBS.

The enhanced BFC stability of the system described here was based on the three following reasons. First, the performance can be effectively maintained by inducing electron transfer between electrocatalytic enzymes and redox mediators immobilized on fuel cell electrodes. All trapped enzymes and redox mediators are activated in the yarn electrode with structural advantage, accentuated by the layer by layer structure [18] which is made by biscrolling method [19], as shown in Fig. 5b (left). This biscrolling structure effectively traps enzymes in the electrode, and plays an important role to enhance the stability of the enzymatic BFC system. Second, the MWNT-based BFC yarn electrode itself was porous and highly electronically conductive providing efficient current collection, and good permeability based on the host material containing PEDOT to act as a bridge between enzymes and electrode surface. Third, conducting polymer, PEDOT, coated on the MWNT sheets by vapor phase polymerization could protect inner layers of the electrode from the outer layers of the electrode surface. These phenomena were described in details with the repulsive force [20] between immobile SO_3^- anionic ions from tosylate-doped PEDOT and chloride ions in body fluids, as shown in Fig. 5b (right). The hydrophilic PEDOT conducting polymer coating on the nanotubes not only enhances nanotube wettability, connectivity, and conductivity [21], but also enhances electrode stability in human body fluid [22]. Therefore electrolyte accessibility is provided within the entire yarn volume, while incorporation of anionic chemical species such as urate, chloride, and ascorbic acid is avoided. Suitable stability in HBS can be attributed to electrostatic interaction that renders the dopant anions relatively immobile in the conducting

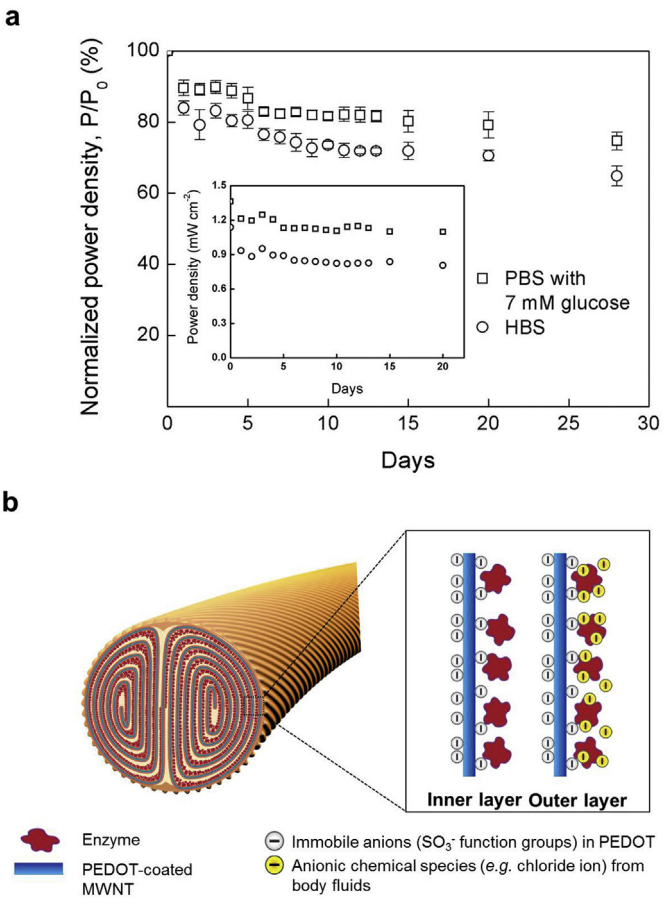

Fig. 5. Enzymatic BFC stability in PBS with 7 mM glucose and HBS. a) Normalized power density (P/P_0, P is the power output of the cells, and P_0 is the initial power output at the starting point of operation) data of BFC system in PBS containing low glucose level (red) and HBS (blue) with stirring, 500 rpm for 20 days. The error bars show the s. d. of normalized power density for three cases. Inset: Experimentally measured power outputs in two operating conditions. b) Schematic illustration of the enzyme-protecting effect of PEDOT layer acting as a cation exchange membrane in the BFC electrode.

polymer. Hence, the PEDOT coating on the MWNTs acts as a cation exchange membrane [22]. As a result, we showed that long-term test of BFC was feasible in low glucose level-containing PBS solution and HBS, and raised the possibilities applying to biomedical devices as potentially implantable BFCs.

4. Conclusions

Here, improved BFC power output and long-term stability performances were demonstrated in low glucose level PBS solution and human body fluid. We showed remarkable power output performance and stability of the full BFC system, exceeding all previous systems to the best of our knowledge, in physiological conditions. We suggested compact, flexible, and easy-handling implantable BFC electrodes. In addition, the influence of biofluid flow rate has been explicitly investigated as is important for real animal/human implantations. These performances are particularly encouraging for harvesting energy by inserting devices inside the human body with internal biomedical devices.

Acknowledgments

This work was supported by the Creative Research Initiative Center for Bio-Artificial Muscle of the Ministry of Education,

Science and Technology (MEST) and the MEST-US Air Force Cooperation Program (Grant No. 2012-00074) in Korea; Air Force Grant AOARD-10-4067, Air Force Office of Scientific Research grant FA9550-12-1-0211, and Robert A. Welch Foundation grant AT-0029 in the USA; and the ARC Centre of Excellence in Electromaterials Science in Australia (Grant No. CE0561616).

Appendix A. Supplementary data

Supplementary data related to this article can be found at http://dx.doi.org/10.1016/j.jpowsour.2015.03.140.

References

[1] A. Heller, Anal. Bioanal. Chem. 385 (2006) 469–473.
[2] J. Kim, K.-H. Yoo, Phys. Chem. Chem. Phys. 15 (2013) 3510–3517.
[3] M. Ammam, J. Fransaer, Biotechnol. Bioeng. 109 (2012) 1601–1609.
[4] C.H. Kwon, S.-H. Lee, Y.-B. Choi, J.A. Lee, S.H. Kim, M.K. Shin, H.-H. Kim, G.M. Spinks, G.G. Wallace, M.D. Lima, M.E. Kozlov, R.H. Baughman, S.J. Kim, Nat. Commun. 5 (3928) (2014) 1–7.
[5] M. Rasmussen, R.E. Ritzmann, I. Lee, A.J. ChloridePollack, D. Scherson, J. Am. Chem. Soc. 134 (2012) 1458–1460.
[6] H. Tsukaguchi, T. Tokui, B. Mackenzie, U.V. Berger, X.-Z. Chen, Y. Wang, R.F. Brubaker, M.A. Hediger, Nature 399 (1999) 70–75.
[7] T. Miyake, S. Yoshino, T. Yamada, K. Hata, M. Nishizawa, J. Am. Chem. Soc. 133 (2011) 5129–5134.
[8] A. Zebda, C. Gondran, A.L. Goff, M. Holzinger, P. Cinquin, S. Cosnier, Nat. Commun. 2 (370) (2011) 1–6.
[9] D. Elad, S. Einav, Standard Handbook of Biomedical Engineering and Design, McGraw-Hill, NY, USA, 2004 (Chapter 3).
[10] D.H. Hussein, H. Gitano-Briggs, M.Z. Addullah, Res. J. Biol. Sci. 4 (2009) 637–643.
[11] S.J. Lee, H.J. Ha, IET Syst. Biol. 7 (2013) 50–55.
[12] K. MacVittie, J. Halámek, L. Halámková, M. Southcott, W.D. Jemison, R. Lobel, E. Katz, Energy Environ. Sci. 6 (2013) 81–86.
[13] N. Mano, A. Heller, J. Electrochem. Soc. 150 (2003) A1136–A1138.
[14] N. Mano, H.-H. Kim, Y. Zhang, A. Heller, J. Am. Chem. Soc. 124 (2002) 6480–6486.
[15] C. Pan, Y. Fang, H. Wu, M. Ahmad, Z. Luo, Q. Li, J. Xie, X. Yan, L. Wu, Z.L. Wang, J. Zhu, Adv. Mater. 22 (2010) 5388–5392.
[16] M. Togo, Y. Yatagawa, M. Oike, H. Kaji, T. Abe, M. Nishizawa, in: Proceedings of Power MEMS, Sendai, Japan, 2008, pp. 65–68.
[17] V. Coman, R. Ludwig, W. Harreither, D. Haltrich, L. Gorton, T. Ruzgas, S. Shleev, Fuel cells 10 (2010) 9–16.
[18] L. Deng, L. Shang, Y. Wang, T. Wang, H. Chen, S. Dong, Electrochem. Commun. 10 (2008) 1012–1015.
[19] M.D. Lima, S. Fang, X. Lepró, C. Lewis, R. Ovalle-Robles, J. Carretero-González, E. Castillo-Martínez, M.E. Kozlov, J. Oh, N. Rawat, C.S. Haines, M.H. Haque, V. Aare, S. Stoughton, A.A. Zakhidov, R.H. Baughman, Science 331 (2011) 51–55.
[20] Y. Tanaka, Russ. J. Electrochem. 48 (2012) 665–681.
[21] J.A. Lee, M.K. Shin, S.H. Kim, S.J. Kim, G.M. Spinks, G.G. Wallace, O.-R. Raquel, M.D. Lima, M.E. Kozlov, R.H. Baughman, ACS Nano 6 (2012) 327–334.
[22] P.S. Tóth, C. Janáky, O. Berkesi, T. Tamm, C. Visy, J. Phys. Chem. B 116 (2012) 5491–5500.